

# Retrieval of Surface Reflectance and Atmospheric Properties Using ASAS Imagery

John V Martonchik and James E. Conel  
Jet Propulsion Laboratory, California Institute of Technology  
Mail Stop 169-237  
4800 Oak Grove Drive  
Pasadena, CA 91109 USA  
T:818.354.2207 F:818.393.4619 Email:jvm@jpl.nasa.gov

## ABSTRACT

Spectral aerosol optical depths and surface hemispherical directional reflectance factors and bihemispherical reflectances are retrieved using multi-angle imagery taken by the airborne Advanced Solid-State Array Spectroradiometer (ASAS). The retrievals were performed using algorithms being devised for use by the Multi-angle Imaging Spectroradiometer (MISR) which will fly on the EOS-AM 1 spacecraft in 1998. As part of its science mission MISR will produce global coverage of both aerosol amounts and surface reflection properties. ASAS imagery are unique datasets for use in testing the efficacy of the MISR retrieval algorithms

## INTRODUCTION

Knowledge of aerosol characteristics and surface spectral reflection properties on a global basis are essential inputs to the study of biospheric and atmospheric climate processes (Charney et al., 1977; Mintz, 1984; Dickinson, 1983). The Multi-angle Imaging Spectroradiometer (MISR) is a radiometrically calibrated instrument, scheduled for launch in 1998 on the EOS-AM 1 platform, which will provide such information in a routine manner (Diner et al., 1993). It has nine CCD array cameras, each with a fixed-view angle at the surface ranging between 70.5° forward and 70.5° aftward, with each camera observing in 4 spectral bands (443, 555, 670 and 865 nm). In its coarse resolution mode the spatial sampling of the imagery will be 1.1 km with a swath width of about 360 km.

To validate the retrieval algorithms which will be used by MISR it is necessary to have access to currently available, comparable, radiometrically calibrated multi-angle imagery. The best such data are those produced by the airborne Advanced Solid-State Array Spectroradiometer (ASAS) (Irons, et al., 1991). Contiguous spectral bands cover the wavelength region 400-1000 nm (and also the MISR bands) and angular coverage currently ranges between 70° forward to 55° aftward. The spatial resolution, however, is considerably better (4 m at a typical observing altitude of 5 km) and the co-registered imagery at the multi-view angles is usually less than 1 km in extent. Therefore, for ASAS data the diffuse radiation component of the measured radiance should be treated as being spatially invariant (pixel independent) over the scene whereas MISR data, with its coarser resolution, can treat this component as being pixel dependent. The retrieval algorithms have been coded to handle both situations.

## ASAS MULTI-ANGLE DATA SET

ASAS made a series of multi-angle images of Bowman Lake in Glacier National Park on 26 February 1992. The lake is at an elevation of 1.25 km and the aircraft flew at an altitude of 4.45 km

ASL with a heading of 235 from true north. The sun was in the west at a zenith angle of 63.4° and an azimuth angle of 214° from true north. Thus, the aircraft was flying into the sun, only about 20° azimuth angle off the principal plane. The 10 view angles were 70, 60, 45, 30 and 15° in the forward direction, nadir, and 15, 30, 45, 55° in the aftward direction. The 559 nm image at forward 30° is shown in Fig. 1. It shows the tip of ice-covered Bowman Lake surrounded by a conifer forest.



Figure 1. ASAS image of Bowman Lake, Glacier NP.

After co-registering the 10 view angle images at each wavelength the resulting 256x256 pixel image set was averaged 4x4 pixels to a final 64x64 pixels data set. This was done in order to 1) minimize co-registration errors, 2) minimize variable footprint size effects at the different view angles, and 3) increase the signal-to-noise ratio. Although the data set contains 29 spectral bands, only those 4 bands closest to the MISR bands were analyzed (ASAS 475, 559, 673, and 866 nm). The averaged image signal-to-noise ratio in the middle two bands was quite good (>100) but that in the 475 and 866 nm bands was markedly less due to lower detector sensitivity. The unaveraged 866 nm band image also had an additional coherent noise problem (noticeable periodic streaking) mitigated somewhat by the averaging procedure.

## RETRIEVAL ANALYSIS

### Aerosol Retrieval

One phase of the aerosol retrieval uses a variation of the technique described by Martonchik and Diner (1992). In the original version

of the technique the images were operated upon by a fast Fourier transform (FFT) to generate view-angle-dependent power spectra as a function of spatial wavenumber. The angular power functions of the non-zero wavenumbers then were used to construct empirical orthogonal functions (or principal components) which described the spatially variable view-angle-dependent surface component of the observed radiance. These empirical orthogonal functions (EOFs) then were used to expand the surface component of the zero wavenumber (image averaged) radiance when an aerosol/atmosphere model is introduced in the analysis. The best estimate of the aerosol/atmosphere condition at the time of the measurements is that model which minimizes the residuals in the expansion procedure involving the EOFs. The variation of the technique used in this study foregoes the FFT and constructs the principal components directly from the radiances associated with the individual pixels in the image.

The second phase of the aerosol retrieval utilizes another, independent, technique which looks for pairs of pixels which have the same (or closely similar) surface reflectance angular shapes but different bihemispherical reflectances (albedos). If such pixel pairs exist, the best estimate of the atmosphere/aerosol condition is that model which can readily identify these pairs. It is not expected that this technique would work for all scene types. One can expect, however, that it would be applicable in those situations where dense, dark vegetation is in the scene on a sub-pixel basis and in variable amounts, thus darkening the reflectance of a fairly homogeneous background somewhat while still retaining the reflectance angular shape of the homogeneous background. This could apply to desert or desert-like areas where variable amounts of vegetative scrub is growing or to the current case in which the 4x4 pixel averaging procedure allows the averaged pixels to contain various amounts of vegetation in those regions along the border of the lake.

The aerosol retrieval results are shown in Fig. 2 for both techniques. An aerosol type was assumed and only the optical depth was retrieved. The aerosol was assumed to be clean-continental, composed mainly of water soluble sulfates and nitrates and a minute part of dust (d'Almeida et al., 1991),

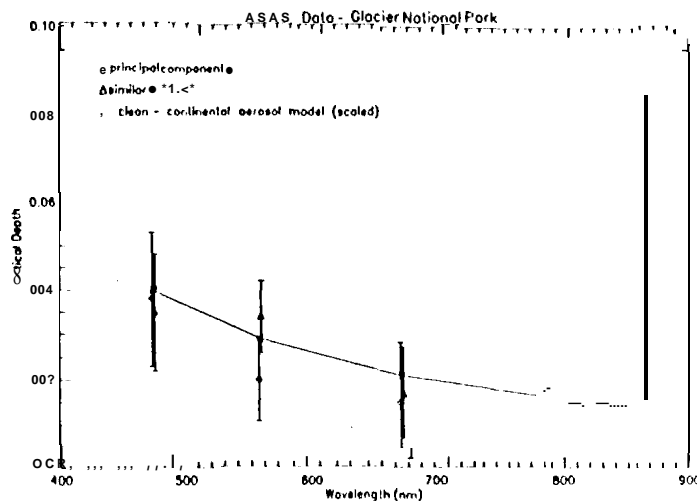


Figure 2. Retrieved aerosol optical depth.

Both techniques give essentially the same optical depth results, about 0.03 at 555 nm. The low optical depth retrieved is consistent with the low radiances observed in the darkest pixels of the image set. Also shown is the spectral dependence of the aerosol model,

scaled to the retrieved optical depths in a least squares sense, illustrating that the assumed model is reasonable. The retrievals at 866 nm show considerably more uncertainty than at the other wavelengths, due to the larger amounts of random and systematic noise in imagery.

#### Surface Retrieval

Once the atmosphere/aerosol properties are known, the surface retrieval is accomplished in a straightforward manner. Since the diffuse radiance at the aircraft level is spatially invariant over the image it is computed first. The technique starts by averaging all the pixels in the scene and retrieving the averaged surface-leaving radiance from the pixel-averaged view-angle-dependent radiances. These radiances are described by a simple integral equation involving the measured radiances, the computed atmospheric quantities, and the unknown averaged surface-leaving radiance. The integral equation can be solved easily for the averaged surface leaving radiance by use of an iteration approach. When the averaged surface-leaving radiance is found, its effect at the observation level then can be computed. This radiation component plus the atmospheric path radiance at the observation level make up the spatially invariant diffuse radiance. The spatially variable surface leaving radiance (multiplied by an exponential atmospheric attenuation transmittance) can then be computed simply by subtracting the diffuse radiance from the measured radiances. These surface-leaving radiances are ratioed to the computed surface leaving radiances for an ideal Lambert surface to produce hemispherical-directional reflectance factors (HDRFs). Integration of these HDRFs over view angle results in bihemispherical reflectances (BHR) or albedo.

Surface HDRF results are shown in Fig. 3 for the conifer forest and in Fig. 4 for the ice-covered lake. The corresponding BHRs are shown in Fig. 5. A number of similar type pixels (i.e., forest or ice) were averaged together and the vertical bars indicate the range in variability.

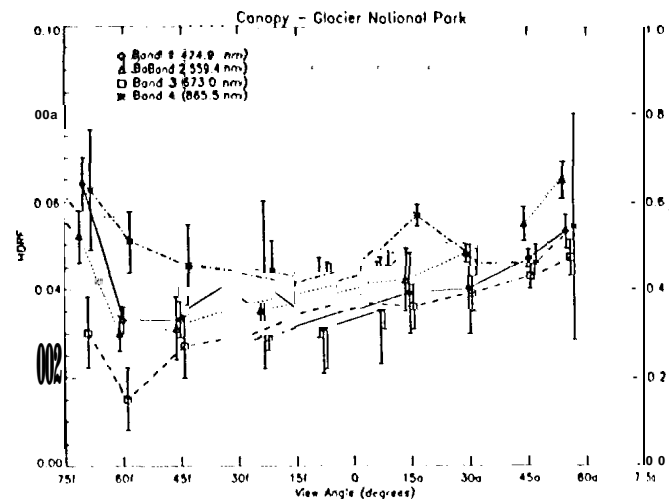


Figure 3. Retrieved HDRFs for conifer canopy. Note the change in scale for the 866 nm band.

The HDRFs for the conifer canopy show the characteristic bow shape, indicative of dense vegetation (Kimes, 1983; Kimes et al., 1985) and the spectral BHRs are typical of dense dark vegetation i.e. dark at visible wavelengths and bright in the near infrared. The HDRFs and BHRs for the ice-covered lake are also typical of snow

(Salomonson and Marlatt, 1968) and may indicate that snow is covering the ice.

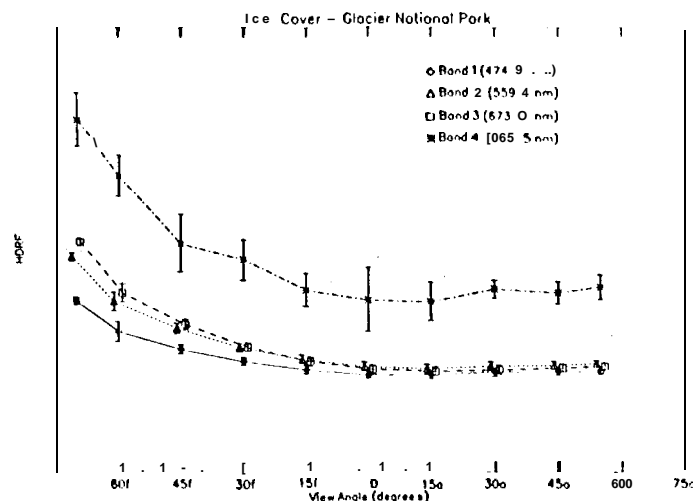


Figure 4. Retrieved HDRF for ice-covered Bowman Lake.

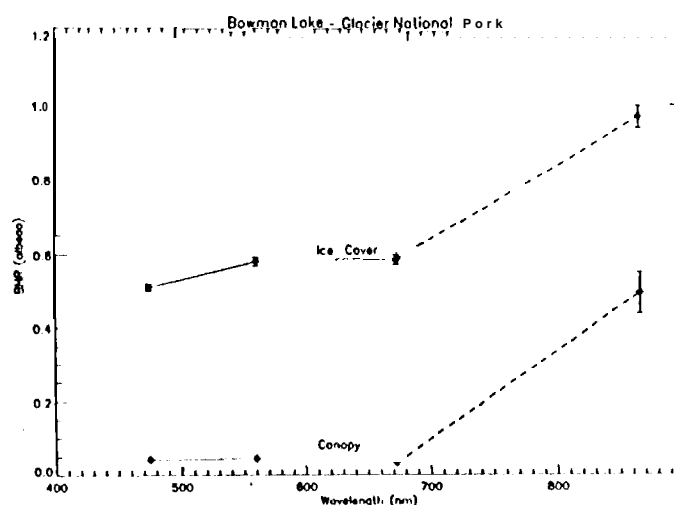


Figure 5. Retrieved BHRs for canopy and lake.

#### ACKNOWLEDGEMENTS

We thank Jim Irons and Dorothy Hall of the Goddard Space Flight Center for providing the ASAS imagery and Lisa Barge and Brian Rheingans for geometrically rectifying and registering the images. We also thank B. Rheingans for the graphical work. This research was performed by the Jet Propulsion Laboratory, California Institute of Technology, under contract with the National Aeronautics and Space Administration.

#### REFERENCES

- d'Almeida, G. A., P. Koepke, and E.P. Shettle, *Atmospheric Aerosols: Global Climatology and Radiative Characteristics*. A. Deepak Publishing, Hampton, VA, 1991.
- Charney, J. G., W.G. Quirk, S.M. Chow, and J. Kornfield, "A Comparative Study of the Effects of Albedo Change of Drought in Semi-arid Regions." *J. Atmos. Sci.* **34** (1977):1366-1385.
- Dickinson, R. E., "Land Surface Processes and Climate-Surface Albedos and Energy Balance." *Adv. Geophys.* **25** (1983):305-353.

Diner, D. J., C.J. Bruegge, T. Deslis, V.G. Ford, L.E. Hovland, D.J. Preston, M.J. Shterenberg, E.B. Villegas, and M. I. White, "Development Status of the EOS Multi-angle Imaging Spectroradiometer (MISR)." *SPIE Proc.* **1939** (1993): 94-103.

Irons, J. R., K.J. Ranson, D.L. Williams, R.R. Irish, and F.G. Huegel, "An Off-nadir-pointing imaging Spectroradiometer for Terrestrial Ecosystem Studies." *IEEE Trans. Geosci. Rem. Sens* **29** (1991): 66-74.

Kimes, D.S., "Dynamics of Directional Reflectance Factor Distributions for Vegetation Canopies." *Appl. Opt.* **22** (1983): 1364-1372.

Kimes, D. S., W.W. Newcomb, R.F. Nelson, and J.B. Schutt, "Directional Reflectance Distributions of a Hardwood and Pine Forest Canopy." *IEEE Trans. Geosci. Remote Sens.* **GE-24** (1985): 281-293.

Martonchik, J.V. and D.J. Diner, "Retrieval of Aerosol Optical Properties from Multi-Angle Satellite Imagery." *IEEE Trans. Geosci. Remote Sensing* **30** (1992): 223-230.

Mintz, Y., "The Sensitivity of Numerically Simulated Climates to Land-Surface Conditions," in *The Global Climate*, ed. J. Houghton, Cambridge, London, New York: Cambridge University Press, 1984.

Salomonson, V.V. and W.E. Marlatt, "Anisotropic Solar Reflectance Over White Sand, Snow and Stratus Cloud," *J. Appl. Meteor.* **7** (1968): 475-483.